

# Large Mass Expansion versus Small Momentum Expansion of Feynman Diagrams

J. Fleischer<sup>1</sup> M. Yu. Kalmykov<sup>2 3 4</sup> and O. L. Veretin<sup>5 6</sup>

*Fakultät für Physik, Universität Bielefeld, D-33615 Bielefeld, Germany.*

## Abstract

The method of the large mass expansion (LME) has the technical advantage that two-loop integrals occur only as bubbles with large masses. In many cases only one large mass occurs. In such cases these integrals are expressible in terms of  $\Gamma$ -functions, i.e. they can be handled completely analytically avoiding even recursions and therefore this approach may find a wide field of application. We consider it necessary to investigate the precision of this method and test it for several two-loop vertex functions occurring in the  $Z \rightarrow b\bar{b}$  decay by comparing it with the small momentum expansion. It turns out that in general high order approximants have to be taken into account for a sufficient accuracy.

*PACS numbers:* 12.15.Ji; 12.15.Lk; 13.40.-b; 12.38.Bx; 11.10.Ji

*Keywords:* Standard Model; Feynman diagram; two-loop diagram; vertex diagram.

---

<sup>1</sup> E-mail: fleischer@physik.uni-bielefeld.de

<sup>2</sup> Bogoliubov Laboratory of Theoretical Physics, Joint Institute for Nuclear Research, 141980, Dubna (Moscow Region), Russia

<sup>3</sup> E-mail: kalmykov@thsun1.jinr.dubna.su

<sup>4</sup> Supported by Volkswagen-Stiftung under I/71 293

<sup>5</sup> E-mail: veretin@physik.uni-bielefeld.de

<sup>6</sup> Supported by BMBF under 05 7BI92P(9)

# 1 Introduction

The experiments at LEP/CERN and SLC/SLAC have reached a precision, which goes beyond all former expectations. It turns out that we are approaching the limits of our theoretical understanding and in order to fully evaluate the present and future experimental data (LEP1 data still to be investigated, LHC and a possible  $e^+e^-$  linear collider) a detailed analysis of higher order corrections is necessary. In particular at higher energies radiative corrections become more and more important since they can grow strongly.

Quite a number of groups have started to develop methods for the evaluation of two-loop diagrams. Analytic results can in general only be obtained for specific mass relations, like e.g. all masses zero or only one non-zero mass in a diagram. Since in the two-loop order for most of the interesting processes the number of diagrams can become of the order of 1000, it is also necessary to calculate these diagrams with extremely high precision for the many different masses occurring in the Standard Model (SM).

A method which provides particular high precision for many kinematical configurations of interest is that of Taylor expansion in an external momentum squared improved by conformal mapping and the Padé summation technique [1]. Another method, which is particularly convenient to program in a formulae manipulating language (we use FORM [2]), is the large mass expansion (LME) [3]. If we have, e.g., diagrams with one large mass like a top-quark in a virtual line [4, 5], the method is shown to be appropriate. To obtain a satisfying precision, however, it turns out to be absolutely necessary that higher order terms of the LME are taken into account. For two-loop propagator-type diagrams such an analysis was carried out in [6]. In this paper we want to consider three-point functions. The particular process we have in mind is  $Z \rightarrow b\bar{b}$ , i.e. we investigate vertex diagrams contributing to this process which contain a top-quark and compare the results of the above two methods in order to find out to what precision it is possible to obtain results from the LME. In most of the cases under consideration the Taylor expansion needs only up to 9 coefficients for a very high precision since we can confine ourselves here to momenta squared below the lowest threshold.

## 2 Large Mass Expansion (LME)

Two-loop diagrams as shown in Fig.1 with two different masses on virtual lines, one of which a top, arise in the process  $Z \rightarrow b\bar{b}$ .  $W$  and  $Z$  are the gauge bosons with masses  $M_W$  and  $M_Z$ , respectively;  $\phi$  is the charged would-be Goldstone boson (we use the Feynman gauge);  $t$  and  $b$  are the t- and b-quarks. In our analysis we neglect the  $b$ -quark mass ( $m_b = 0$ ). Thus we have the following kinematics (see Fig.1):  $p_1^2 = p_2^2 = 0$ ,  $(p_2 - p_1)^2 = q^2$  and  $q^2 = M_Z^2$  for the on-shell  $Z$ . For such type of diagrams analytic results are impossible to obtain with presentday technology.

Applying the method of the LME,  $M_W$  and  $M_Z$  are considered as small. In the framework of this expansion contributions from additional subgraphs are to be taken into account together with the Taylor expansion of the initial diagrams w.r.t. external momenta and light masses. These subgraphs restore the analytic properties of the initial diagrams (like logarithmic behaviour). In other words, the Taylor expansion of the initial

diagrams produces extra infrared singularities which are compensated by singularities of the additional subgraphs so that only the singularities of the original diagrams survive.

For a given scalar graph  $\Gamma$  the expansion in the large mass is given by the formula [3]

$$F_\Gamma(q, M, m, \varepsilon) \stackrel{M \rightarrow \infty}{\sim} \sum_\gamma F_{\Gamma/\gamma}(q, m, \varepsilon) \circ T_{q^\gamma, m^\gamma} F_\gamma(q^\gamma, M, m^\gamma, \varepsilon), \quad (1)$$

where  $\gamma$ 's are subgraphs involved in the LME,  $\Gamma/\gamma$  denotes shrinking of  $\gamma$  to a point;  $F_\gamma$  is the Feynman integrand corresponding to  $\gamma$ ;  $T_{q^\gamma, m^\gamma}$  is the Taylor operator expanding this integrand in small masses  $\{m_\gamma\}$  and external momenta  $\{q_\gamma\}$  of the subgraph  $\gamma$ ;  $\circ$  stands for the convolution of the subgraph expansion with the integrand  $F_{\Gamma/\gamma}$ . The sum goes over all subgraphs  $\gamma$  which (a) contain all lines with large masses, and (b) are one-particle irreducible w.r.t. light lines.

At this point it becomes clear what the difference is between the small- $q^2$  expansion and what is called here the LME: in the former case we assume all masses large, i.e.  $q^2 \ll M_W^2, M_Z^2, m_t^2$  while in the latter case only  $m_t$  is considered as large and all other parameters small, i.e.  $q^2, M_W^2, M_Z^2 \ll m_t^2$ . In this sense both methods are LM expansions. The technical advantage of the second method is, however, that only bubbles with one mass occur, which can be expressed in terms of  $\Gamma$  functions, while in the case of the small  $q^2$  expansion bubbles with different masses are involved, which are much more difficult to evaluate. Of course also the number and structure of the subgraphs is different in the two cases.

The structure of the LME of the diagrams under consideration is given in Fig.2. Bold, thin and dashed lines correspond to heavy-mass, light-mass, and massless propagators, respectively. Dotted lines indicate the lines omitted in the original graph  $\Gamma$  to yield the subgraph  $\gamma$ .  $\Gamma/\gamma$  (see (1)) then consists out of all the dotted lines after shrinking  $\gamma$  to a point. Thus, in case 0 the last and in case N the two last contributions vanish in dimensional regularization. Finally the LME of the above diagrams has the following general form:

$$F_{\text{as}}^N = \frac{1}{m_t^4} \sum_{n=-1}^N \sum_{i,j=-1; i+j=n}^n \left( \frac{M_W^2}{m_t^2} \right)^i \left( \frac{q^2}{m_t^2} \right)^j \sum_{k=0}^m A_{i,j,k}(q^2, M_W^2, \mu^2) \ln^k \frac{m_t^2}{\mu^2} \quad (2)$$

where  $m$  is the highest degree of divergence (ultraviolet, infrared, collinear) in the various contributions to the LME ( $m \leq 3$  in the cases considered).  $M_W^2/m_t^2$  and  $q^2/m_t^2$  are considered as small parameters.  $A_{i,j,k}$  are in general complicated functions of the arguments, i.e. they may contain logarithms and higher polylogarithms (see also the explicit examples below). (2) implies that the difference  $F - F_{\text{as}}^N$  of the integral  $F$  and its approximation behaves like

$$F - F_{\text{as}}^N = O \left( \frac{(M_W^2)^i (q^2)^j \ln^m \frac{m_t^2}{\mu^2}}{(m_t^2)^{N+2}} \right), \quad \text{with } i + j = N. \quad (3)$$

One might expect this difference to indicate the order of the real error of the asymptotic expansion. For  $q^2$  small this will indeed be the case, for  $q^2 \simeq M_Z^2$  the ‘‘small’’ parameters are not really small anymore and the validity of the LME can only be inferred from

the comparison with results from other methods, for which we take here the small  $q^2$  expansion. In particular nothing can be said about a range of convergence of the LME. We can, however, at least formally apply the Padé approximation method to improve the convergence, the encouraging results of which will be demonstrated below.

### 3 Results

The small momentum expansion of cases 7, 7.1 and 7.2 (notation due to FST of [1]) is described in detail in Ref. [7]. The additional subgraph arising in these cases is the same irrespectively of the mass distribution and is shown in Fig.2 (case 7).

In the case of the LME two additional subgraphs arise in each of the cases 7.1 and 7.2. Beyond that these sets of additional subgraphs are also of quite different structure. Furthermore the 2<sup>nd</sup> and 4<sup>th</sup> graphs in the row (see Fig.2) produce  $1/\varepsilon^3$  terms which cancel, however. Since there are no UV divergences, these must be mixtures of infrared and collinear ones. They determine the highest degree of divergence in these cases and thus the highest power of the logarithm as discussed in (2).

Our numerical results for cases 7.1 and 7.2 are presented in Fig.3, and for  $q^2 = M_Z^2$  in Table 1. In the figures we show the small  $q^2$ -expansion in comparison with the lowest order approximation and the sum of terms with  $N=9$ , see (2). The scale parameter  $\mu = m_t$ , i.e. only  $k=0$  contributes in (2). We see that up to  $q^2 = M_Z^2$  the sum of 11 terms agrees quite well with the small  $q^2$ -expansion, while for higher  $q^2$  the agreement very quickly worsens. For this reason we formally apply also the Padé summation technique. With 11 terms in the series, a [5/5]-approximant (long-dashed) can be constructed. It is seen that indeed this improves the situation considerably up to the first threshold though for a better agreement many more terms in the LME would be needed. In the small  $q^2$ -expansion only 9 terms were taken into account, i.e. a [4/4] approximant is calculated. The high precision of the results in this case even up to the threshold (in case 7.2) is due to the mapping applied in addition (see [1]). From Table 1 we see that for  $q^2 = M_Z^2$  indeed a rather precise result can be obtained with 11 terms from the LME, in particular if Padé's are applied.

In case 0 an extremely high agreement between the small- $q^2$  expansion and the LME is obtained (see Table 1). No deviation in a figure like above would be seen.

The last two cases: A (for asymmetric) and N (for nonplanar) are difficult from the point of view of the small  $q^2$ -expansion. While for the planar and symmetric diagrams a "standard" numerical program was written (applied e.g. in [7]), this program is not without considerable changes applicable for an asymmetric diagram and not without even more extensions for a nonplanar one. Thus in these cases just the analytic expressions for the first 9 Taylor coefficients of the small  $q^2$ -expansion were produced with FORM in terms of bubble integrals and then numerically evaluated. The problem is that higher coefficients get quite lengthy in this manner so that the FORTRAN programs are difficult even to compile (in the multiple precision version of D. H. Bailey [8])!

In case N the lowest threshold is indeed quite high and therefore the obtained coefficients yield an extremely precise result for the diagram at  $q^2 = M_Z^2$ . What concerns the LME, the situation is essentially the same as in cases 7.1 and 7.2 (see Fig.3 and Table 1).

Case A is interesting due to the fact that the lowest threshold is right at  $q^2 = M_Z^2$  (in fact the singular contribution at this point should cancel against some Bremsstrahlung contribution to the  $Z \rightarrow b\bar{b}$  decay). Table 2 demonstrates that in this case the LME yields results of extremely high precision, which perfectly agree with the results from the small- $q^2$  expansion at low  $q^2$ . Near and above the threshold, however, the precision of the small  $q^2$ -expansion with a total of 9 coefficients is getting worse, but nevertheless the agreement is still quite surprising. In this case, obviously, the LME is superior to the small momentum expansion.

$F^{(0)}$  in Tables 1 and 2 corresponds to the lowest order of the diagrams (N=-1 or 0, respectively) and  $F^{(4)}$  to the order of expansion performed in Ref. [9].

Table 1: Values of diagrams at  $q^2 = 90^2$ ,  $\mu = m_t = 180$ ,  $M_W = 80$ .

	$J_{7.1}$		$J_{7.2}$		$J_0$	$J_N$
$F^{(0)}$	6.4	-i30.0	9.2	-i24.5	0.64	-1.5
$F^{(4)}$	11.1	-i17.93	9.4	-i44.848	0.45750	-0.86
$F^{(10)}$	10.1	-i17.95218	10.122	-i44.84523	0.457525	-0.718
[5/5]	9.996	-i17.9528	10.189	-i44.842	0.457523132	-0.7031
small- $q$	9.992668259	-i17.95215366	10.193902102	-i44.845273975	0.4575231327	-0.7026099843

Table 2: Case A for different  $q^2$ .

$q^2/M_Z^2$	0.1	0.9	1.1		2.0	
$F^{(0)}$	-0.324	-1.36	-0.067	-i2.17	0.463	-i0.408
$F^{(10)}$	-0.3431585700	-1.438044241	-0.089798389	-i2.290275185	0.48623819	-i0.449860818
small- $q$	-0.3431585700	-1.4378	-0.093	-i2.25	0.482	-i0.445

## Acknowledgment

We want to thank A. Kotikov and V. Smirnov for fruitful discussions. M.Yu.K. is grateful to the Volkswagen Stiftung and O.V. to BMBF for financial support. Both are grateful to the Physics Department of the University of Bielefeld for the warm hospitality.

## A Analytical Expressions

In this section we present the first two terms of the LME for the diagrams under consideration. All Feynman integrals are normalised as follows

$$\frac{(4\pi)^{2\varepsilon}}{(16\pi^2)^2 M^4} \frac{\Gamma^2(1+\varepsilon)\Gamma^2(1-\varepsilon)}{\Gamma(1-2\varepsilon)} J = \mu^{4\varepsilon} \int \frac{d^d k_1}{i(2\pi)^d} \frac{d^d k_2}{i(2\pi)^d} \frac{1}{D_1 D_2 D_3 D_4 D_5 D_6}, \quad (4)$$

where  $D_i = (q_i^2 - m_i^2)$  are corresponding inverse propagators and  $d = 4 - 2\varepsilon$  is the space-time dimension. Instead of the large mass  $M$ , the small mass  $m$  and the momentum squared,  $q^2$ , we introduce the dimensionless parameters  $z = m^2/M^2$  and  $s = q^2/m^2$  and write the results of the LME as a series in  $z$  with each coefficient being  $s$ -dependent.

$$zsJ_{7.1} = -\frac{1}{\varepsilon^2} - \frac{1}{\varepsilon}(-L_q - L_M + 1) - \frac{1}{2}(L_q + L_M)^2 + (L_q + L_M) - 1 \\ - z \left[ \left( \frac{1}{\varepsilon^2} - \frac{1}{\varepsilon}L_q + \frac{1}{2}L_q^2 \right) \left( L_m - L_M + \frac{12+s}{12} \right) \right]$$

$$\begin{aligned}
& + \left( \frac{1}{\varepsilon} - L_q \right) \left( \frac{1}{2} (L_M^2 - L_m^2) - \frac{24+s}{12} L_M + L_m + \frac{8-3s}{8} \right) + \frac{1}{6} (L_m^3 - L_M^3) \\
& - \frac{1}{2} L_m^2 + \frac{24+s}{24} L_M^2 - \frac{s}{2} L_q + L_m + \frac{7s-16}{8} L_M + \frac{16-23s}{16} \Big] + O(z^2), \quad (5)
\end{aligned}$$

$$\begin{aligned}
zsJ_{7.2} = & - \left( \frac{1}{\varepsilon^2} - \frac{1}{\varepsilon} L_q + \frac{1}{2} L_q^2 \right) (L_M - L_m + I_1(s) - 1) \\
& - \left( \frac{1}{\varepsilon} - L_q \right) \left( \frac{1}{2} L_m^2 - \frac{1}{2} L_M^2 + L_M - I_1(s) L_m + I_2(s) - 1 \right) - \frac{1}{6} (L_M^3 - L_m^3) \\
& + \frac{1}{2} L_M^2 - L_M - \frac{1}{2} I_1(s) L_m^2 + I_2(s) L_m - I_3(s) + 1 + O(z), \quad (6)
\end{aligned}$$

$$J_0 = -1 + \zeta(2) - z \left[ L_M - L_m + \frac{144+49s}{72} - \frac{4+s}{2} \zeta(2) \right] + O(z^2), \quad (7)$$

$$\begin{aligned}
zsJ_A = & + \frac{1}{2\varepsilon} \log(1-s) - \frac{1}{2} \left( (L_m + L_M) \log(1-s) + \log^2(1-s) + \text{Li}_2(s) \right) \\
& - z \left[ -\frac{1}{24\varepsilon} \left( (1+s) \log(1-s) + s \right) - \frac{s}{24} L_m + \frac{s}{8} L_M + \frac{s}{18} \right. \\
& \left. + \frac{1+s}{24} \left( (L_m + L_M - 1) \log(1-s) + \log^2(1-s) + \text{Li}_2(s) \right) \right] + O(z^2), \quad (8)
\end{aligned}$$

$$\begin{aligned}
J_N = & -\frac{1}{2\varepsilon} - \frac{3}{2} + L_M - z \left[ \frac{1}{\varepsilon} \left( L_m - L_M + \frac{72+7s}{48} \right) - \frac{1}{2} L_m^2 - L_m L_M \right. \\
& \left. + \frac{3}{2} L_M^2 + 3L_m - \frac{144+7s}{24} L_M + \frac{720+181s}{288} + 2\zeta(2) \right] + O(z^2), \quad (9)
\end{aligned}$$

where  $L_M = \log(M^2/\mu^2)$ ,  $L_m = \log(m^2/\mu^2)$  and  $L_q = \log(-q^2/\mu^2)$  with  $\mu$  being an arbitrary scale parameter. The functions  $I_n(s)$  can be expressed in terms of polylogarithms  $\text{Li}_k$ . Here we give only their integral representations

$$I_n(s) = \frac{1}{2} \frac{(-)^n}{n!} \int_0^1 \frac{\log^n(1-ts/4)}{\sqrt{1-t}} dt. \quad (10)$$

## References

- [1] J. Fleischer and O.V. Tarasov, *Z.Phys.***C64** (1994) 413; J. Fleischer, *Int.J.Mod.Phys.***C6** (1995) 495; J. Fleischer, V. A. Smirnov and O. V. Tarasov, *Z.Phys.***C74** (1997) 379.
- [2] J.A.M. Vermaseren, *Symbolic manipulation with FORM*, Amsterdam, Computer Algebra Nederland, 1991.
- [3] F.V. Tkachov, Preprint INR P-0332, Moscow (1983); P-0358, Moscow 1984; K.G. Chetyrkin, *Teor. Math. Phys.* **75** (1988) 26; *ibid* **76** (1988) 207; Preprint, MPI-PAE/PTh-13/91, Munich (1991); V.A. Smirnov, *Comm. Math. Phys.***134** (1990) 109; *Renormalization and Asymptotic Expansions*, Birkhäuser, Basel, 1991.

- [4] J. Fleischer, O.V. Tarasov, F. Jegerlehner and P. Rączka, Phys. Lett.**B293** (1992) 437; G. Buchalla and A.J. Buras, Nucl. Phys.**B398** (1993) 285; G. Degrossi, Nucl. Phys.**B407** (1993) 271; K.G. Chetyrkin, A. Kwiatkowski and M. Steinhauser, Mod. Phys. Lett.**A8** (1993) 2785.
- [5] J. Fleischer, O.V. Tarasov, F. Jegerlehner, Phys. Lett.**B293** (1992) 437;
- [6] A.I. Davydychev, V.A. Smirnov and J.B. Tausk, Nucl. Phys.**B410** (1993) 325; F.A. Berends, A.I. Davydychev, V.A. Smirnov and J.B. Tausk, Nucl. Phys.**B439** (1995) 536; F.A. Berends, A.I. Davydychev and V.A. Smirnov, Nucl. Phys.**B478** (1996) 59; L.V. Avdeev and M.Yu. Kalmykov, Nucl. Phys.**B502** (1997) 419; G. Weiglein, hep-ph/9711254.
- [7] J. Fleischer et al., hep-ph/9704353, to be published in Z.Phys.**C**.
- [8] D.H. Bailey, ACM Transactions on Mathematical Software, **19** (1993) 288.
- [9] R. Harlander, T. Seidensticker and M. Steinhauser, hep-ph/9712228, preprint MPI/PhT/97-81, TTP97-52.

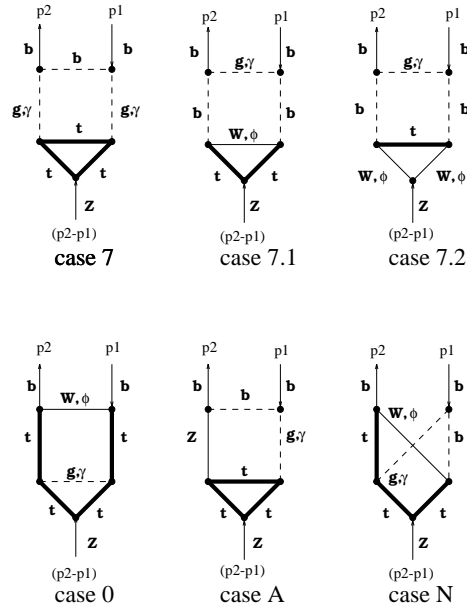


Figure 1: Two-loop diagrams with two different masses in internal lines arising in the process  $Z \rightarrow b\bar{b}$ .

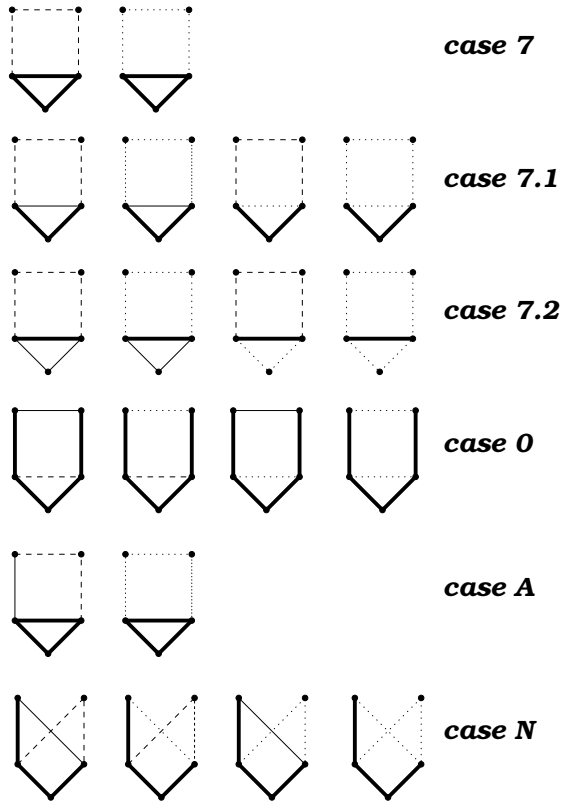


Figure 2: The structure of the LME, see explanations in the text.

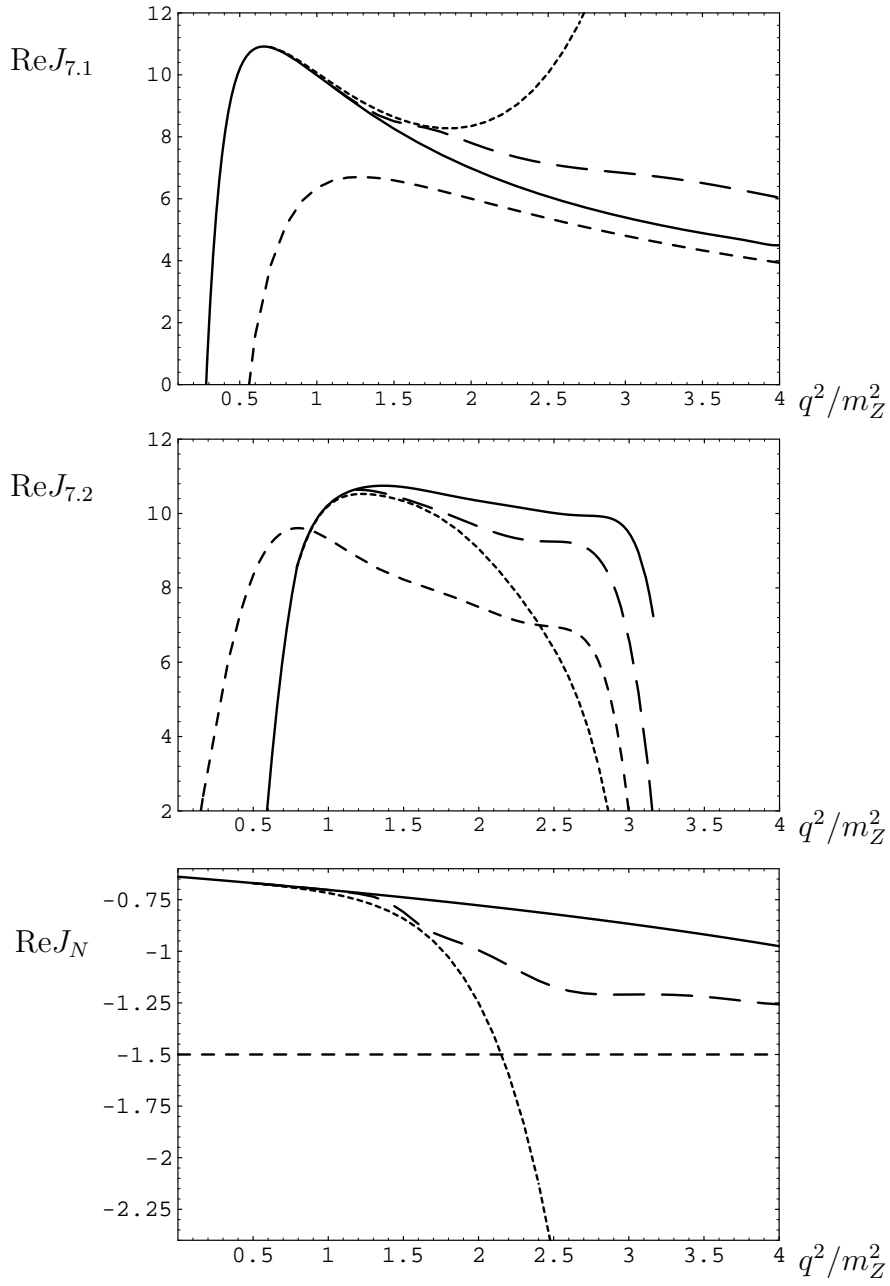


Figure 3: Results of the LME for the real finite parts of diagrams 7.1, 7.2 and N with  $\mu^2 = m_t^2$ . Solid curves represent the small- $q^2$  expansions, middle-dashed the leading term of the LME, short-dashed the sum of 11 terms in the LME, long-dashed the [5/5] Padé approximant from the LME.